

DOI:10.1002/ejic.201500273

Structural and Magnetic Analysis of Retrosynthetically Designed Architectures Built from a Triply Bridged Heterometallic (CuL)₂Co Node and Benzenedicarboxylates

Soumavo Ghosh,^[a] Guillem Aromí,^[b] Patrick Gamez,^[b,c] and Ashutosh Ghosh^{*[a]}

Keywords: Schiff bases / Heterometallic complexes / Bridging ligands / Coordination polymers / Magnetic properties

The flexible trinuclear metallatecton [(CuL)₂Co]²⁺ [H₂L = *N,N'*-bis(salicylidene)-1,3-propanediamine] has been used as a building block, and its coordinative interaction with *ortho*-, *meta*-, and *para*-benzenedicarboxylates (BDCs) has been investigated to evaluate the positional isomeric effect of these carboxylate ligands on the resulting compounds. Structural characterization reveals that *o*-H₂BDC produces a discrete trinuclear complex, namely [(CuL)₂Co(*o*-HBDC)₂]·H₂O (**1**). As expected from the retrosynthetic design, one-dimensional (1D) coordination polymers, i.e., [(CuL)₂Co(*m*-BDC)]·CH₃OH]_∞ (**2**) and [(CuL)₂Co(*p*-BDC)]·2CH₃OH]_∞ (**3**), are obtained with *m*-BDC and *p*-BDC linkers, respectively. In all three complexes, the triply bridged bimetallic trinuclear coordination clusters are linear and solely a *syn-syn* bridging mode is observed for the carboxylates. In **2**, the nodes are connected sidewise and are inclined toward each other to be

accommodated by the 120°-angular *m*-BDC units, whereas in **3**, the linear *p*-BDC linkers connect the parallel nodes diagonally. These differences in connectivity give rise to one-dimensional "great wall"-like chains for **2** and to quasi-linear coordination chains for **3**. These distinct one-dimensional propagations induced by the different BDC isomers influence the three-dimensional columnar packing of **2** and **3**. Magnetic susceptibility measurements and fitting of the results confirm that these three compounds are made by analogous magnetic building blocks, with very similar antiferromagnetic intramolecular magnetic exchange (with *J* in the −16.96 to −11.80 cm^{−1} range, using the −2*JS*₁*S*₂ convention). The structural homogeneity of the magnetic fragment within this family of compounds has allowed magnetostructural correlations to be explored, which has not previously been attempted.

Introduction

One of the most significant advances that has revolutionized synthetic chemistry in the second half of the 20th century was the combinatorial assembly of small molecular building blocks of complementary functionalities under specific conditions to generate more intricate, finite, or infinite architectures of different dimensions.^[1] This applies from conventional organic or inorganic chemistry to current macromolecular (modules and connectors) or supramolecular chemistry (nodes and spacers).^[2] The predictability of supramolecular architectures that are formed by using organic modules based on a covalent frame is superior to inorganic nodes involving noncovalent interactions, which

often leads to random processes.^[3] From the synthetic point of view, the design of molecular building blocks that will allow a higher rate of predictability is one of the crucial challenges of modern metallosupramolecular chemistry.^[4]

To confine the directionality of a metallic node, the use of discrete complexes of various nuclearities as metallatectons in combination with exodentate organic ligands (spacers) has been the foremost strategy to obtain predictable architectures.^[5] In such cases, the influence of a specific stereochemical preference of a spacer used for a particular tecton is undeniable. The use of spacers with monoatomic donating sites (e.g., N-donor spacers) has been highly successful in this regard.^[6] On the other hand, spacers with polycarboxylate donating sites often show unpredictable results because they can exhibit more than one type of stereochemical orientation to their complementary tecton. Polycarboxylate spacers are well known for inducing such unpredictability (Scheme 1);^[7] such compounds even adjust their ligating properties through accommodation of the geometric disposition of the carboxylate functionalities around an organic tecton (e.g., BDCs), which is often termed a positional isomeric effect.^[8] However, the positional isomeric effect should strictly be defined as the architectural changes that arise solely from a particular geometrical disposition

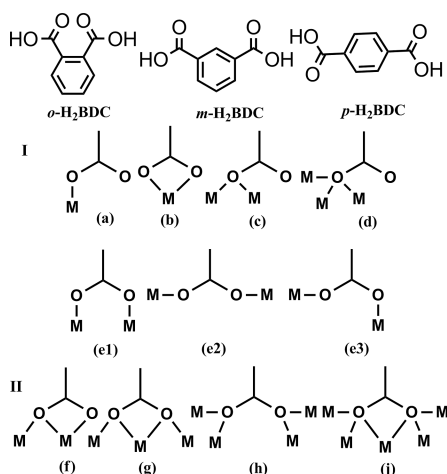
[a] Department of Chemistry, University College of Science, University of Calcutta, 92, A.P.C. Road, Kolkata 700009, India
E-mail: ghosh_59@yahoo.com
http://173.201.183.21/~cuchemistry/?page_id=439

[b] Departament de Química Inorgànica, Universitat de Barcelona, Martí i Franquès 1–11, 08028 Barcelona, Spain

[c] Institució Catalana de Recerca i Estudis Avançats (ICREA), Passeig Lluís Companys 23, 08010 Barcelona, Spain

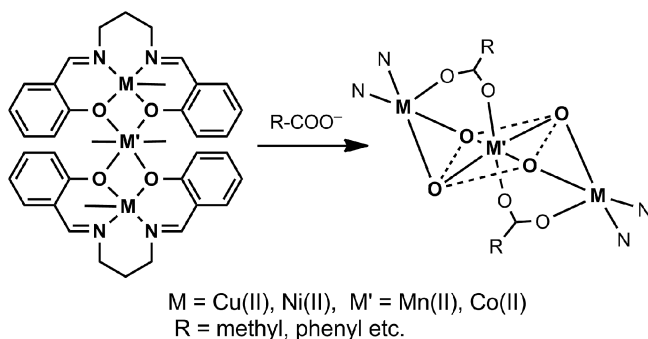
Supporting information for this article is available on the WWW under <http://dx.doi.org/10.1002/ejic.201500273>.

of the donating atoms, without changing the coordination mode to a particular tecton. Such a crucial distinction has been largely overlooked for polycarboxylates.



Scheme 1. Representation of the different H_2BDC isomers and the various coordination modes of monocarboxylates.

Besides the spacer itself, the metallatecton can also play a very important role in controlling the stereochemical preferences of the spacer around the available coordination sites of a node.^[5a,9] The positional isomeric effect has mainly been studied with mononuclear nodes;^[8] examples involving polynuclear nodes are rare, most likely because of the higher complexity of ligation around these.^[10] For instance, similar dinuclear nodes with different polycarboxylato ligand backbones^[11] and metal combinations^[12] may produce entirely different architectures that would depend on the symmetry, steric demand, conformational or coordinative flexibility etc. of the metallatecton. For trinuclear $[(\text{ML})_2\text{M}']$ clusters ($\text{H}_2\text{L} = \text{salen-type Schiff base}$), it has recently been found that these species can adopt a symmetrical linear conformation that only permits a *syn-syn* bridging mode; apparently, irrespective of the metal ions (Scheme 2).^[13] Therefore, such trinuclear nodes potentially represent ideal systems to investigate the positional isomeric effect of benzene dicarboxylates. Such a study has not yet been reported, although metallatectons derived from Robson-type macrocycles, bicompartamental N_2O_4 - and N,N,O -donor ligands have been tested previously in this regard.^[5b]



Scheme 2. $[(\text{ML})_2\text{M}']$ clusters ($\text{H}_2\text{L} = \text{salen-type Schiff base}$).

One-dimensional coordination polymers (CPs)^[14] obtained from distinct BDC isomers (Scheme 1) provide an exceptional platform from which to establish magnetic correlation for heterometallic clusters, as long as the nodes satisfy non-nil-spin ground state at low temperatures.^[8b,15] Very recently, we studied discrete $(\text{ML})_2\text{M}'$ single-atom bridged spin-coupled systems with axially bridged carboxylates that showed interesting magnetic properties.^[13,16] Although one can envisage joining such trinuclear tectons using polycarboxylates (Scheme 2), to our knowledge, no studies involving such a strategy have been described. Heterometallic $\text{Cu}^{\text{II}}/\text{Co}^{\text{II}}$ systems are expected to exhibit intricate magnetic properties as a result of considerable orbital and spin-orbit coupling contributions to the effective magnetic moment arising from the intrinsic orbital angular momentum in the octahedral ground state of high-spin Co^{II} ions $[\text{4T}_{1\text{g}}(\text{F})]$.^[17,18] A few structurally and magnetically characterized 1D/2D/3D CPs containing heterometallic diphenoxido-bridged $\text{Cu}^{\text{II}}/\text{Co}^{\text{II}}$ nodes have been reported,^[11b,19] and most of these are constructed with binuclear nodes derived from compartmental ligands with various spacers.

In the present study, we report on the synthesis, characterization, crystal structures, and magnetic properties of three $[(\text{Cu}^{\text{II}})_2\text{Co}^{\text{II}}]$ complexes [$\text{H}_2\text{L} = \text{N,N}'\text{-bis(salicylidene)-1,3-propanediamine}$], namely the discrete trinuclear complex $[(\text{CuL})_2\text{Co}(\text{o-HBDC})_2] \cdot \text{H}_2\text{O}$ (**1**), and two 1D coordination polymers $\{[(\text{CuL})_2\text{Co}(\text{m-BDC})] \cdot \text{CH}_3\text{OH}\}_\infty$ (**2**) and $\{[(\text{CuL})_2\text{Co}(\text{p-BDC})] \cdot 2\text{CH}_3\text{OH}\}_\infty$ (**3**). Complexes **2** and **3** represent very rare cases of rationally designed connectivity between triply bridged bimetallic trinuclear nodes in one-dimension,^[20a] although such connections in serendipitous assemblies of homometallic MOFs are common.^[20b,20c,20d] The results show a significant modulation of the connectivity, architectures, and 3D packing; yet, the relative positions within the linear $\text{Cu}^{\text{II}}\text{--Co}^{\text{II}}\text{--Cu}^{\text{II}}$ triads are fixed, with similar $\text{Cu}^{\text{II}}\text{--O--Co}^{\text{II}}$ angles. However, slight changes in angles give rise to small variations in the magnitude of the antiferromagnetic exchange interactions in these complexes, enabling a possible magnetostructural correlation to be drawn.

Results and Discussion

Synthesis and Spectral Characterization

Recently, we successfully synthesized several discrete and polymeric $[(\text{ML})_2\text{M}']$ -type complexes (where, M represents Cu^{II} and Ni^{II} , and M' are different s-, p-, d-, and f-block elements).^[21] In these polymeric complexes, neutral or anionic N-donor spacers that connect the $(\text{ML})_2\text{M}'$ tectons through bis-/tris-monodentate modes were used.^[21c,21d,21e] The flexibility of the molecular building blocks plays a crucial role in the formation of isomeric coordination polymers. In our present endeavor, we have used carboxylato spacers for the first time with this type of metallatectons with the objective of quenching their flexibility and generating linear structures. To limit the flexibility factor of the

spacers, we have used different geometric isomers of the rigid BDCs, to achieve structure predictability. All three complexes were obtained as light-green crystals upon mixing the required precursors in methanol at room temperature, followed by slow evaporation of the solvent. The conformational adaptability and quenched flexibility of the linear trinuclear $[(\text{Cu}^{\text{II}}\text{L})_2\text{Co}^{\text{II}}]^{2+}$ coordination cluster^[13a] distinguishes polyatomic carboxylate functionalities at the axial positions, and permits solely a *syn-syn* bridging mode of ligation of the three isomeric BDCs. However, the singly protonated phthalate produces a discrete trinuclear complex, whereas isophthalate and terephthalate offer rare one-dimensional chains of the same metallic core.

In addition to elemental analyses, all the complexes were initially characterized by their IR spectra. The precursor metalloligand $[\text{CuL}]$ is neutral (i.e., it does not have a counter anion), whereas all three complexes contain IR-active carboxylate co-ligands. The carboxylate anion shows characteristic bands for bidentate chelation in each compound.^[22] In all complexes, a strong and sharp band ascribed to the azomethine $\nu(\text{C}=\text{N})$ group of the Schiff base appears at $1620\text{--}1624\text{ cm}^{-1}$ for $[\text{CuL}]$, as observed earlier.^[22c]

All three complexes and the free metalloligand have been characterized by UV/Vis spectroscopy in acetonitrile as well as in the solid state. In solution, all compounds display very similar UV/Vis spectra, with intense bands at approximately 365 (ligand-to-metal charge-transfer transition of $[\text{CuL}]$), 272, and 230 nm (intraligand $n\text{--}\pi^*$ and $\pi\text{--}\pi^*$ transitions of $[\text{CuL}]$), which are similar to those of the free metalloligand (see the Supporting Information, Figure S1, left). The solid-state electronic spectra exhibit small shifts of the d–d transition bands of the metalloligand, as a result of its complexation with the Co^{II} center (see the Supporting Information, Figure S1, right). Hence, the corresponding band at 598 nm for the free $[\text{CuL}]$ moiety is observed at 590 (**1**), 615 (**2**), and 612 nm (**3**), whereas the charge-transfer bands are found at 384 nm for **1**, and at 380 nm for **2** and **3**.

Description of the Structures

Structure of **1**

The X-ray crystal structure of **1** (Figure 1) consists of a linear^[13a] trinuclear unit, $[(\text{CuL})_2\text{Co}(\text{o-HBDC})_2]\cdot\text{H}_2\text{O}$ (*o*-HBDC stands for singly deprotonated phthalic acid). Selected coordination bonds and angles are listed in Table 1.

The structure of complex **1** includes a hexacoordinate central cobalt(II) atom in a CoO_6 octahedral geometry together with two pentacoordinate square-pyramidal copper(II) atoms from two $[\text{CuL}]$ metalloligands. Two bridging phenoxido oxygen atoms from each $[\text{CuL}]$, i.e., O(1) and O(2), and O(5) and O(6) form the equatorial plane of the CoO_6 unit, with bond lengths of $2.059(4)\text{--}2.085(4)\text{ \AA}$. The axial positions are occupied by the oxygen atoms O(3) and O(7) of the *syn-syn* bridging carboxylato ligands ($1\kappa\text{O}:2\kappa\text{O}'$) belonging to two monoanionic phthalates, with bond lengths of $2.144(5)$ and $2.146(5)\text{ \AA}$, respectively. The

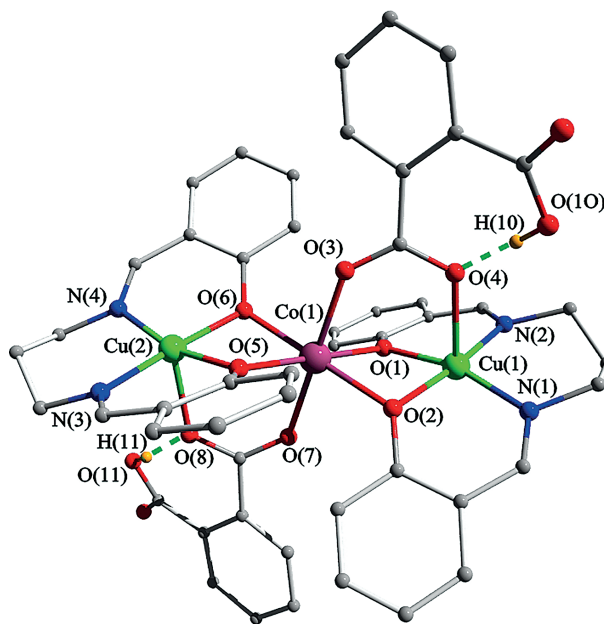


Figure 1. Representation of the molecular structure of **1** together with a partial atomic numbering scheme. Hydrogen atoms attached to carbon and solvent molecules are omitted for clarity; Co (pink), Cu (light-green), O (red), N (blue), C (gray), H (orange); intramolecular hydrogen bonding shown in dark-green.

bond lengths of the ligating atoms to the Co^{II} center in **1** are comparable with those reported for CoO_6 elongated octahedra exhibiting weak Jahn–Teller distortion, a typical feature for high-spin Co^{II} ions. The *cis* angles with the axially coordinated atoms [in the range of $88.5(2)\text{--}91.7(2)^\circ$] as well as the *trans* angles [in the range of $179.3(2)\text{--}179.8(2)^\circ$] are close to the ideal values (90 and 180° , respectively), but the *cis* angles in the equatorial plane [in the range of $75.3(2)\text{--}105.1(2)^\circ$] deviate considerably, and are thus indicative of a distorted octahedral geometry. The terminal Cu(1) and Cu(2) atoms are pentacoordinate in a square-pyramidal coordination geometry. The basal planes of each of the two terminal copper atoms contain four donor atoms of the Schiff base; namely, two imine N atoms [N(1), N(2) for Cu(1) and N(3), N(4) for Cu(2)] with Cu–N bond lengths in the range $1.963(7)\text{--}1.984(5)\text{ \AA}$, and two phenoxido O atoms [O(1), O(2) for Cu(1) and O(5), O(6) for Cu(2)] with Cu–O bond lengths in the range $1.945(5)\text{--}1.955(5)\text{ \AA}$. The bridging carboxylato groups occupy the axial positions of the square pyramids with Cu(1)–O(4) and Cu(2)–O(8) distances of $2.301(5)$ and $2.282(5)\text{ \AA}$, respectively. The angles between the axially and basally coordinated atoms of the square-pyramidal Cu centers vary within a narrow range of $90.3(3)\text{--}98.0(3)^\circ$. The so-called Addison parameter (τ_5) amounts to 0.132 and 0.116 for Cu(1) and Cu(2), respectively, which confirms the slightly distorted square-pyramidal geometry for the copper(II) ions (τ_5 is 0 for a perfect square pyramid, whereas it has a value of 1 for a trigonal bipyramid).^[23] The r.m.s. deviations of the four basally coordinated donor atoms from the mean planes are 0.107 and 0.088 \AA for Cu(1) and Cu(2), respectively, with the metal

Table 1. Selected bond lengths [Å] and angles [°] for complexes **1–3**.^[a]

	1	2	3
Cu(1)–O(1)	1.945(5)	1.959(6)	1.951(3)
Cu(1)–O(2)	1.955(5)	1.950(6)	1.970(4)
Cu(1)–O(4)	2.301(5)	2.197(7)	2.290(4)
Cu(1)–N(1)	1.982(8)	1.986(7)	1.988(5)
Cu(1)–N(2)	1.963(7)	1.993(9)	1.978(4)
Cu(2)–O(5)	1.951(4)	1.933(6)	–
Cu(2)–O(6)	1.950(5)	1.971(6)	–
Cu(2)–O(8)	2.282(5)	2.182(7)	–
Cu(2)–N(3)	1.970(6)	1.998(9)	–
Cu(2)–N(4)	1.984(5)	1.961(8)	–
Co(1)–O(1)	2.075(5)	2.138(6)	2.079(4)
Co(1)–O(2)	2.085(4)	2.118(7)	2.137(3)
Co(1)–O(3)	2.144(5)	2.059(6)	2.090(4)
Co(1)/Co(2) ^[b] –O(5)	2.066(5)	2.127(6)	–
Co(1)/Co(2) ^[b] –O(6)	2.059(4)	2.088(5)	–
Co(1)/Co(2) ^[b] –O(7)	2.146(5)	2.079(6)	–
O(1)–Cu(1)–O(2)	81.3(2)	81.6(3)	81.9(1)
O(1)–Cu(1)–O(4)	96.4(2)	95.4(2)	92.1(1)
O(1)–Cu(1)–N(1)	90.6(3)	90.6(3)	91.6(2)
O(1)–Cu(1)–N(2)	163.9(3)	167.5(3)	166.4(2)
O(2)–Cu(1)–O(4)	90.8(2)	93.9(3)	92.5(1)
O(2)–Cu(1)–N(1)	171.9(3)	167.1(3)	164.8(2)
O(2)–Cu(1)–N(2)	90.3(2)	89.9(3)	89.9(2)
O(4)–Cu(1)–N(1)	90.3(3)	97.1(3)	101.5(2)
O(4)–Cu(1)–N(2)	97.4(2)	94.3(3)	99.0(2)
N(1)–Cu(1)–N(2)	97.5(3)	96.1(3)	93.7 (2)
O(5)–Cu(2)–O(6)	80.7(2)	81.2(2)	–
O(5)–Cu(2)–O(8)	94.8(2)	96.6(3)	–
O(5)–Cu(2)–N(3)	91.5(2)	90.8(3)	–
O(5)–Cu(2)–N(4)	165.0(3)	167.8(3)	–
O(6)–Cu(2)–O(8)	91.3(2)	96.5(3)	–
O(6)–Cu(2)–N(3)	172.0(2)	169.9(3)	–
O(6)–Cu(2)–N(4)	91.3(3)	90.8(3)	–
O(8)–Cu(2)–N(3)	90.9(2)	90.4(3)	–
O(8)–Cu(2)–N(4)	98.0(3)	93.4(3)	–
N(3)–Cu(2)–N(4)	96.0(3)	96.1(3)	–
O(1)–Co(1)–O(2)	75.3(2)	73.8(2)	75.1(1)
O(1)–Co(1)–O(3)	91.1(2)	90.1(2)	87.8(1)
O(1)–Co(1)–O(5)/O(1a)/O(1b)	179.3(2)	180.00	180.00
O(1)–Co(1)–O(6)/O(2a)/O(2b)	105.1(2)	106.3(2)	104.9(1)
O(1)–Co(1)–O(7)/O(3a)/O(3b)	88.6(2)	89.9(2)	92.2(1)
O(2)–Co(1)–O(3)	89.9 (2)	88.8(2)	90.7(1)
O(2)–Co(1)–O(5)	104.1(2)	–	–
O(2)–Co(1)–O(6)	179.4(2)	–	–
O(2)–Co(1)–O(7)/O(3a)/O(3b)	90.0(2)	91.2(2)	89.3(1)
O(3)–Co(1)–O(5)	88.5(2)	–	–
O(3)–Co(1)–O(6)	89.6(2)	–	–
O(3)–Co(1)–O(7)	179.8(2)	–	–
O(5)–Co(1)–O(6)	75.5(2)	–	–
O(5)–Co(1)–O(7)	91.7(2)	–	–
O(6)–Co(1)–O(7)	90.5 (2)	–	–
O(5)–Co(2)–O(6)	–	74.1(2)	–
O(5)–Co(2)–O(7)	–	90.8(2)	–
O(5)–Co(2)–O(5a)	–	180.00	–
O(5)–Co(2)–O(6a)	–	105.9(2)	–
O(5)–Co(2)–O(7a)	–	89.2(2)	–
O(6)–Co(2)–O(7)	–	89.1(2)	–
O(6)–Co(2)–O(7a)	–	90.9(2)	–

[a] Symmetry codes: a: 2 – x, –y, 1 – z; b: –x, 2 – y, –z for complexes **2** and **3**, respectively. [b] Co(1) for complexes **1** and **3** and Co(2) for complex **2**.

atoms located at 0.127(1) and 0.130(1) Å away from the plane, towards O(4) and O(8) atoms, respectively.^[13a]

The heterometallic coordination cluster in **1** is comprised of one cobalt octahedron and two copper square pyramids

joined together through two monoatomic and one triatomic bridges, in an edge-sharing manner. Previous reports state that [(ML)₂M']-type tectons usually play multiple roles in the self-assembly because of their inherent flexibility in the presence of co-ligands with monoatomic donating sites.^[21] However, carboxylates quench the flexibility of these tectons, generating *linear* systems through their *syn–syn* bridging mode. Hence, the two carboxylato ligands bind to the metallatecton in an *anti* fashion so that the coordination cluster can be considered as “Z-shaped”. *o*-HBDC is a “60°-angular-type” organic tecton that is expected to join [(CuL)₂Co] metallatectons at both ends of the “Z” to produce a 1D chain, although, one end of the “60°-angular-tecton” is not engaged in coordination, and instead remains protonated (and participates in an intramolecular hydrogen bond). Consequently, the complex is a discrete trinuclear entity. All attempts to deprotonate the second carboxylic acid group of *o*-HBDC to favor the formation of a 1D chain led to the rupture the metallatectons, producing a [Co(*o*-BDC)] MOF; presumably the chelate effect of the (*o*-BDC)^{2–} anion at higher pH values [pK_{a2}(*o*-H₂BDC) >> pK_{a1}(*o*-H₂BDC)], together with a likely steric impediment, prevents the polymerization of the trinuclear cluster, giving rise to its dissociation.

The crystal packing of **1** shows the presence of a disordered water molecule in the interstitial spaces of the supramolecular assembly, with 50% occupancy at each site nearer to the protonated carboxylic acid groups. Molecules of **1** pack closely to generate a 1D supramolecular column along the crystallographic *c*-axis by means of moderate C(8)–H(8A)⋯O(12) interactions (symmetry code: 1 – x, –y, –1/2 + z), with H⋯O and C(H)⋯O contact distances of 2.69(1) and 3.47(1) Å, respectively, and ∠C–H⋯O of 138(1)° (see the Supporting Information, Figure S2).

Structures of **2** and **3**

The X-ray crystal structures of **2** and **3** consist of centrosymmetric linear trinuclear coordination clusters (see Figures 2 and 3) of formulae [(CuL)₂Co(BDC)] (BDC stands for doubly deprotonated benzenedicarboxylate and it represents isophthalate, i.e., *m*-BDC, for **2** and terephthalate, i.e., *p*-BDC for **3**), where the Co^{II} ion sits at a center of symmetry. Selected coordination bonds and angles are listed in Table 1.

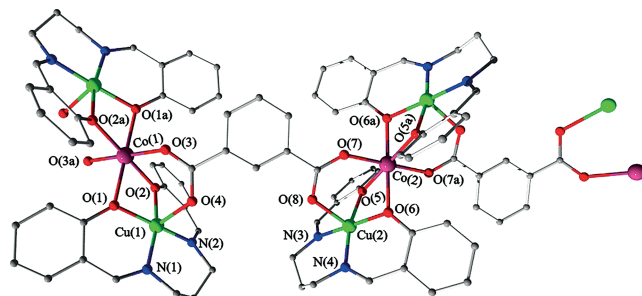


Figure 2. Representation of the molecular structure of **2** together with a partial atomic numbering scheme. Hydrogen atoms and solvent molecules are omitted for clarity; color scheme as indicated in Figure 1.

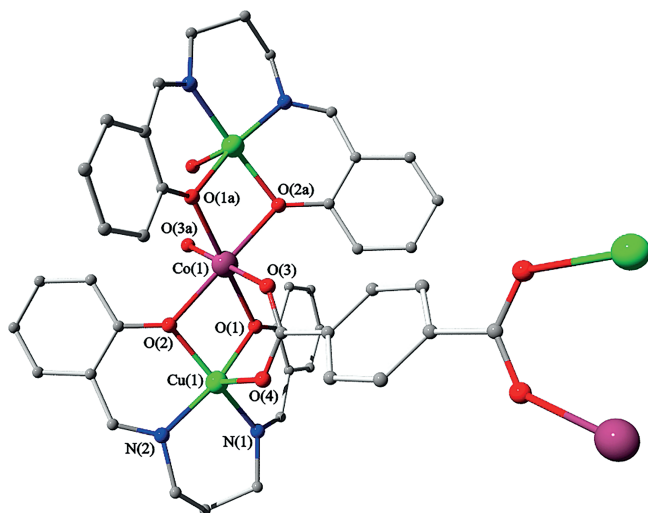


Figure 3. Molecular structure of **3** together with a partial atomic numbering scheme. Hydrogen atoms and solvent molecules are omitted for clarity; color scheme as indicated in Figure 1.

The asymmetric unit of $\{[(\text{CuL})_2\text{Co}(m\text{-BDC})]_n\}$ (**2**) contains two halves of $(\text{CuL})_2\text{Co}$ units connected by two carboxylate ($1\kappa\text{O}:2\kappa\text{O}'$) groups from one *m*-BDC acting as *syn-syn* bridging ligand (Figure 2). The structures of the trinuclear units are comparable, with slight differences in bond lengths and angles. They are formed by a hexacoordinate central cobalt(II) atom in a CoO_6 octahedral geometry and two pentacoordinate square-pyramidal copper(II) atoms from two $[\text{CuL}]$ metalloligands. For each Co atom, two pairs of bridging phenoxido O atoms from two metalloligands [for Co(1); O(1), O(2), O(1a), O(2a), for Co(2); O(5), O(6), O(5a), O(6a)] are in a planar arrangement. Two additional O atoms, normal to this plane, from *m*-BDC linkers [for Co(1); O(3), O(3a) and for Co(2); O(4), O(4a)] complete the CoO_6 octahedron. The Co(1) octahedron is slightly compressed [$\text{Co(1)}\text{--O(3)}_{\text{ax}}$: 2.059(6) Å; $\text{Co(1)}\text{--O}_{\text{eq}}$: 2.138(6) and 2.118(7) Å], whereas the Co(2) octahedron is slightly elongated [$\text{Co(2)}\text{--O(5)}_{\text{ax}}$: 2.127(6); $\text{Co(2)}\text{--O}_{\text{eq}}$: 2.088(5) and 2.079(6) Å], thus indicating a weak Jahn–Teller distortion. The distortions of the *cis* and *trans* angles of the Co octahedron are analogous to those of **1**. The two symmetrically related Cu atoms reside in a five-coordinate square-pyramidal coordination space, as observed for **1**, where the basal plane is formed by an asymmetric N_2O_2 donor set from a Schiff-base ligand, the axial position being occupied by a $\mu_{1,3}$ -bridging carboxylato group (Table 1). The Cu–N and Cu–O bond lengths are comparable with those of **1**. The τ_5 values amount to 0.007 and 0.035, for Cu(1) and Cu(2), respectively. The r.m.s. deviations of the four basally coordinated donor atoms from the mean plane of the pentacoordinate Cu(1) and Cu(2) atoms in **2** are 0.009 and 0.023 Å, with the metal atoms being 0.178(1) and 0.140(1) Å away from the plane, respectively, toward the atoms O(4) and O(8).

Compound $\{[(\text{CuL})_2\text{Co}(p\text{-BDC})]_n\}$ (**3**) displays centers of symmetry at the Co atom and at the ring centroid of the *p*-BDC linker (Figure 3). Hence, its asymmetric unit con-

sists of half of the trinuclear unit. The $[(\text{CuL})_2\text{Co}]$ coordination cluster is equivalent to that in **2**, with two pairs of bridging phenoxido O atoms from two $[\text{CuL}]$ metalloligands [O(1) and O(2); O(1a) and O(2a)] in a planar arrangement around the CoO_6 octahedron, and two carboxylato O atoms [O(3) and O(3a)] at the axial positions. The bond parameters around the Co coordination sphere are similar to those found in **1** and **2**, with a weak Jahn–Teller distortion [$\text{Co(1)}\text{--O(2)}_{\text{ax}}$: 2.137(3) Å; $\text{Co(1)}\text{--O}_{\text{eq}}$: 2.079(4) and 2.090(4) Å] of the octahedral geometry. The symmetrically related Cu atoms from each metalloligand adopt a five-coordinate square-pyramidal geometry, with an asymmetric N_2O_2 basal plane [O(1), O(2), N(1) and N(2)], and an oxygen atom, i.e., O(4), from a $\mu_{1,3}$ -bridging carboxylato group at the axial position. The bond parameters of the Cu centers are comparable with those of **1** and **2**. The τ_5 value amounts to 0.027. The r.m.s. deviation from the mean plane of the four basally coordinated donor atoms of the pentacoordinate Cu(1) is 0.022 Å, with the metal atom being 0.224(1) Å away from the plane, towards the atom O(4).

The archetype of $[(\text{ML})_2\text{M}']$ clusters ($\text{M} = \text{Cu}^{\text{II}}$ and $\text{M}' = \text{Co}^{\text{II}}$) in **2** and **3** remain unaltered as in **1**; that is, displaying a “Z-shape” with very small differences in the phenoxido bridging angles (Table 2). The variations in the structures are due to the different orientation of the carboxylate group of the BDC linkers (Figure 4). For **2**, the triply bridged trinuclear nodes are inclined toward each other to be accommodated by the 120° -angular dicarboxylate linkers, generating a 1D “great wall”-like coordination chain along the crystallographic *c*-axis (Figure 4, top).^[24] This assembly represents a rare case of heterometallic coordination polymers involving isophthalic acid.^[25] For **3**, the linear linkers keep the nodes parallel to each other to build up a 1D quasi-linear coordination chain along the crystallographic *c*-axis (Figure 4, bottom).^[26] In both cases, the coordination modes of the complementary building blocks are identical; the distinct chain propagations are due to the skeletal disposition of the chemical functionality of the organic tectons.

Table 2. List of $\mu_{1,1}$ bridging angles for complexes **1–3**.

$\mu_{1,1}$ Bridging angle	1	2	3
Cu(1)–O(1)–Co(1)	98.3(2)	97.6(3)	99.6(1)
Cu(1)–O(2)–Co(1)	97.6(2)	98.6(3)	97.0(1)
Cu(2)–O(5)–Co(1)/Co(2) ^[a]	98.0(2)	97.2(3)	–
Cu(2)–O(6)–Co(1)/Co(2) ^[a]	98.3(2)	97.3(2)	–

[a] Co(1) for complex **1** and Co(2) for complex **2**.

For both **2** and **3**, the adjacent chains run parallel to form a 2D grid structure through π – π stacking (4.8 and 3.8 Å for **2** and **3**, respectively) and C–H \cdots π interactions, which are common features in solid-state structures of molecules containing aromatic moieties. These layers are further stacked into a 3D framework through C–H \cdots π and C–H \cdots O interactions, with supramolecular voids containing solvent molecules. In **2**, the relative tilting of the tectons with a planar *m*-BDC creates a void that can accommodate one methanol molecule. In the case of **3**, the *p*-BDC is

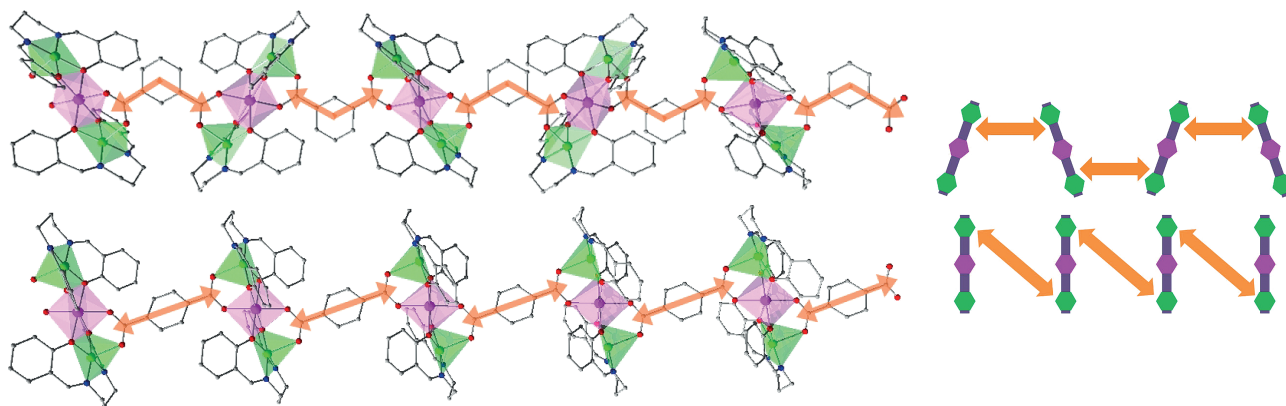
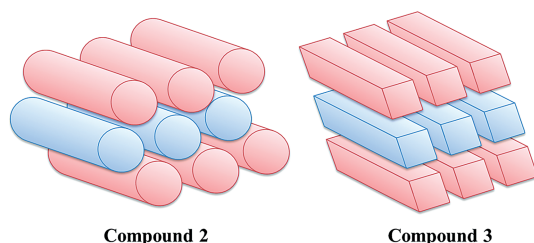


Figure 4. 1D packing diagrams (left panel) of **2** (top) and **3** (bottom), along the crystallographic *c*-axis, and their schematic representations (right panel).

twisted, which leads to an increase in the void space that can accommodate two methanol molecules. The solid-state packing of **2** and **3** are significantly different (Scheme 3). The 1D chains of **2** display a hexagonal columnar packing, whereas closely packed tetragonal columns are observed for **3**.^[27]



Scheme 3. 3D packing diagrams of **2** (hexagonal columnar packing: left) and **3** (tetragonal columnar packing: right), with 1D columns along the crystallographic *c*-axis.

Polycarboxylate linkers can show diverse and irregular connecting modes that usually lead to unpredictable and often undesirable architectural changes, thus frustrating a systematic control of structural features.^[9] In the present study, the carboxylate functionalities interact with the metal centers only through a *syn-syn* bridging mode, as anticipated, and, depending on the relative disposition of the functionalities, they assemble in a discrete or 1D fashion, with a different connectivity and packing. Evidently, the systematic and rather predictable behavior exhibited by this symmetric metallatecton illustrates its exceptional adaptability to isomeric dicarboxylates with different shapes. Such prediction and evaluation of positional isomeric effect of any organic tecton on bimetallic polynuclear nodes is very rare.^[10a] The generation of heterometallic trinuclear nodes with dicarboxylate entities had been accomplished previously through serendipitous assembly under solvothermal conditions, which do not allow the consequent architectures to be predicted.^[20] Although, a few isolated reports of connecting homometallic Cu₂O₂ and Ni₂O₂ tectons with BDCs that can be correlated as positional isomeric effect have been described.^[28,29]

It should be noted that a small number of symmetric dinuclear metallatectons are known for which di- or tricarboxylates coordinate only in a bis- or tris-(*syn-syn* bidentate) mode.^[11a,30] In asymmetric heterodinuclear tectons, the coordination modes of the dicarboxylates are usually unpredictable.^[11b,19b] However, such unpredictability is greatly diminished by the use of symmetric linear trinuclear tectons that only allow a bis(*syn-syn* bidantate) mode for the dimerization.^[31] These trinuclear tectons are derived from bi-compartmental N₂O₄ Schiff bases, which provide an extremely stable coordination core that blocks most of the coordination sites of the central metal atom. Therefore, for further networking, a coordination number of at least eight is required for the central metal atom. In contrast, the use of N₂O₂ Schiff bases offers fewer blocking possibilities of coordination sites of the central metal atom, at the expense of a lower stability of the coordination core. As a result, the robustness of such types of metal clusters is reduced, making them very difficult to employ as nodes. Here, for the first time, we succeeded in connecting this type of complex with isomeric BDCs, ensuring that their donor functionalities remain unchanged, which led to extremely rare 1D bimetallic chains of triply bridged trinuclear nodes.

Magnetic Properties

Complexes **1–3** add to the growing family of identified heterometallic Cu^{II}/Co^{II} complexes. The study of their magnetic properties is complicated by the simultaneous presence of magnetic exchange together with the contribution of the orbital angular momentum of high-spin octahedral Co^{II}. This can be done by a matrix diagonalization procedure employing a magnetic Hamiltonian that considers the spin-orbit coupling within the Co^{II} ion, the exchange between the spin angular momenta, and the Zeeman interaction of the various magnetic moments of the system with the magnetic field (see below).

Magnetization measurements at variable temperature (2 to 300 K) under a constant magnetic field (0.5 T) were collected on microcrystalline samples of **1–3**; the results are

presented in Figure 5 as $\chi_M T$ vs. T plots (χ_M is the molar paramagnetic susceptibility). In all cases, the $\chi_M T$ product is above the expected value for the spin only value expected for two Cu^{II} ions ($S = 1/2$) and one Co^{II} high spin center ($S = 3/2$), all magnetically dilute (3.51, 3.63, and $3.71 \text{ cm}^3 \text{ K mol}^{-1}$ for **1**, **2**, and **3**, respectively; expected value $2.63 \text{ cm}^3 \text{ K mol}^{-1}$ for all $g = 2$). The reason is the influence of the orbital angular momentum of Co^{II} , $L = 1$, on the overall magnetic susceptibility of the system.

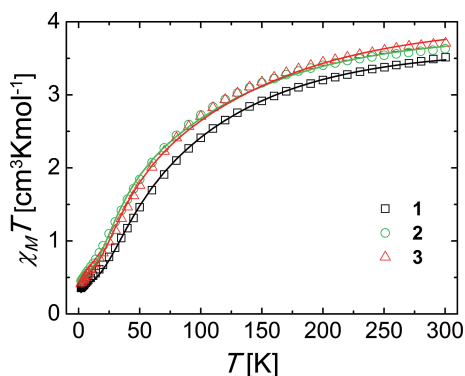


Figure 5. Plots of $\chi_M T$ vs. T for complexes **1**, **2**, and **3**. The solid lines are fits to the experimental data (see text for details).

The program PHI^[32] was employed to fit the experimental data by diagonalization of the Hamiltonian in Equation (1).

$$H^{\wedge} = \lambda \sigma L^{\wedge}_1 \hat{S}_1 - 2J(\hat{S}_1 \hat{S}_2 + \hat{S}_1 \hat{S}_3) + \mu_B(\sigma L^{\wedge}_1 + g_1 \hat{S}_1 + g_2 \hat{S}_2 + g_3 \hat{S}_3)B \quad (1)$$

In this Hamiltonian, L^{\wedge} and \hat{S}_1 are isotropic orbital and spin angular momenta of Co^{II} , respectively, whereas \hat{S}_2 and \hat{S}_3 are the spin operators of the two copper ions in one molecule. Likewise, g_1 , g_2 , and g_3 are isotropic gyromagnetic ratios of these three metals, respectively, with terms J , λ , and σ corresponding, respectively, to the $\text{Co}^{\text{II}}\text{--Cu}$ exchange-coupling constant, the Co spin-orbit coupling constant, and a combined orbital reduction parameter of this metal.^[33] The terms μ_B and B are the Bohr magneton and the external magnetic field, respectively. This model does not include any intermolecular interactions because it is assumed from the structural data that the coupling between clusters is negligible; thus the three compounds were treated in exactly the same manner.

This fitting methodology was previously employed for an analogous series of $[\text{Cu}^{\text{II}}\text{--Co}^{\text{II}}\text{--Cu}^{\text{II}}]$ molecular clusters;^[13a] therefore, for the purpose of comparison, we used the same set of fixed parameters employed before. Thus, reasonable values of 2.0 and 2.2 were employed for g_1 and $g_2 = g_3$, respectively, and $\lambda = 180 \text{ cm}^{-1}$ was employed for all the compounds. In addition, optimal fittings were obtained by including contributions by small amounts of Co^{II} paramagnetic impurities (amounting to 0.122, 0.18, and 0.18 molar fraction for **1**, **2**, and **3**, respectively). The best solutions were obtained for J and σ values for **1/2/3** of $-16.96/-11.80/-13.53 \text{ cm}^{-1}$ and $-1.37/-1.54/-1.67$, respectively; the resulting simulation curves are represented as solid lines in Figure 5. The moderate coupling, together with the effect of the paramagnetic impurities prevent the observation of clear max-

ima in the χ_M vs. T plots. The model used also provides good fittings of these plots (see the Supporting Information, Figure S3).

The parameters obtained through this calculation are similar to those of the previously studied analogue, also featuring single *syn,syn*-carboxylate bridges between Cu and Co, in addition to the two μ_2 -phenoxide ligands. In a previous paper we unveiled an approximate correlation between the average $[\text{Cu--O--Co}]$ angle in bis- μ_2 -phenoxide systems and the magnitude of the coupling constant J . The significant dispersion of this correlation is due to the large number of other variables that also have an influence on this property. We here report three compounds with the same molecular skeleton as that of the previously reported compound $[(\text{CuL})_2\text{Co}(\text{OBz})_2]$ ($\text{OBz} = \text{benzoate}$).^[13a] Possible magnetostructural correlations within this small family of very similar analogues were thus investigated. Surprisingly, important distortions were encountered in the attempts to correlate J with the average $[\text{Cu--O--Co}]$ angle. The possibility for the largest or the smallest angle within the bridged moiety to have more weight than the other was then investigated. We found a much better correlation by using the smallest angle for each compound, which seems then to play a more important role than the other (see the Supporting Information, Figure S4).

The contribution of spin-orbit coupling prevents the definition of a total spin ground state for this molecule. However, Co^{II} clusters with orbital angular momentum have shown slow relaxation of the magnetization (for example, see Zhang et al.^[34]). Therefore, AC magnetic susceptibility measurements were performed for clusters **1**, **2**, and **3**. No sign of an out-of-phase component of the magnetization could be observed, even for the largest frequency.

Conclusions

By utilizing the tactical advantage of the particular coordinative interaction and adaptability of the $[(\text{ML})_2\text{M}']$ coordination cluster towards carboxylate functionalities, herein, we assess the positional isomeric effect of three benzenedicarboxylates towards a trinuclear heterometallic metallatecton for the first time. As expected from a retrosynthetic view, the combinatorial self-assembly of complementary building blocks led to the formation of rare 1D-coordination polymers consisting of $[(\text{Cu}^{\text{II}}\text{L})_2\text{Co}^{\text{II}}]$ nodes and *m*-BDC and *p*-BDC linkers for **2** and **3**, respectively. On the other hand, *o*-BDC persists in its singly protonated form to constitute a discrete complex **1**. Although **2** and **3** have the same constitutional formulae, except for solvent content, the relative differences of the angularity of *m*-BDC and *p*-BDC isomers change the propagation from “great wall”-like for **2** to quasi-linear for **3** along with 3D-supramolecular columnar packing. Such changes in connectivity, propagation, and packing attributed only to the geometrical disposition of the chemical functionality in BDCs as the coordinating mode of carboxylate remains unaltered in all three complexes. From the magnetic point of view, these structures are practically monomeric where the intramolecular magnetic exchange coupling constants J are found to be -16.96 , -11.80 , and -13.53 cm^{-1} for complexes **1**, **2**, and **3**, respectively. A possible magneto-struc-

tural correlation suggests that the smaller oxido bridging angle for each compound might play a more important role than the larger angle for lowering the antiferromagnetic interaction.

Experimental Section

Starting Materials: Salicylaldehyde and 1,3-propanediamine were obtained from Spectrochem India, and were of reagent grade and used as received. The reagents and solvents used were of commercially available reagent quality, unless otherwise stated.

Caution! Perchlorate salts of metal complexes with organic ligands are potentially explosive. Only a small amount of material should be prepared and it should be handled with care.

Synthesis of the Schiff-Base Ligand H₂L and the Metalloligand [CuL]: The di-Schiff-base ligand H₂L was synthesized by following reported methods.^[35] 1,3-Propanediamine (5 mmol, 0.42 mL) was mixed with salicylaldehyde (10 mmol, 1.05 mL) in methanol (20 mL). The resulting solution was heated to reflux for ca. 2 h, and subsequently cooled to room temperature. The yellow methanolic solution was used directly for complex formation. To a methanolic solution (20 mL) of Cu(ClO₄)₂·6H₂O (1.852 g, 5 mmol), a methanolic solution of H₂L (5 mmol, 20 mL) and triethylamine (1.4 mL, 10 mmol) were added to prepare the respective precursor “metalloligand” [CuL].^[35]

{[(CuL)₂Co(o-HBDC)]·H₂O} (1): To a methanolic solution (20 mL) of the precursor metalloligand [CuL] (0.359 g, 1 mmol), a solution of Co(ClO₄)₂·6H₂O (0.183 g, 0.5 mmol) in methanol (2 mL) was added and the mixture was stirred for 5 min. In another portion, phthalic acid (0.166 g, 1 mmol) was dissolved in methanol (3 mL), and triethylamine (138 µL, 1 mmol) was added. The phthalic acid solution was added slowly to the mixture of metalloligand and Co(ClO₄)₂ with vigorous stirring for 1 h. The mixture was filtered and left undisturbed for slow evaporation of the solvent. After ca. three days, crystals of X-ray quality appeared at the bottom of the vessel. The crystalline compound was collected, washed with cold methanol, air dried, and characterized by elemental analysis, spectroscopic methods, and X-ray diffraction.

Compound 1: Yield 0.345 g (63%). C₅₀H₄₄CoCu₂N₄O₁₃ (1094.92): calcd. C 54.85, H 4.05, N 5.12; found C 54.77, H 4.11, N 5.08. UV/Vis: λ_{max} (MeCN, absorbance) = 360, 270, 231 nm; λ_{max} (solid, reflectance) = 590, 384 nm. IR (KBr): ν_{s+as}(COO[−]) = 1553, 1370, ν(C=N) = 1620 cm^{−1}.

{[(CuL)₂Co(m-BDC)]·CH₃OH}_n (2) and {[(CuL)₂Co(p-BDC)]·2CH₃OH}_n (3): To a solution of the precursor metalloligand [CuL] (0.036 g, 0.1 mmol) in methanol (20 mL), a solution of Co(ClO₄)₂·6H₂O (0.018 g, 0.05 mmol, 5 mL of methanol) was added and the solution was stirred for 5 min. An aqueous solution (5 mL) of the disodium salt of *m*-BDC or *p*-BDC (0.010 g of each, 0.05 mmol) was added dropwise with stirring, for **2** and **3**, respectively. A green precipitate immediately appeared. The mixture was stirred for 2.5 h, and subsequently filtered to remove any residue. The clear filtrate was allowed to stand overnight at room temperature for slow evaporation of the solvent, and crystals of X-ray quality appeared at the bottom of each vessel.

Compound 2: Yield 0.025 g (53%). C₄₃H₄₀CoCu₂N₄O₉ (942.82): calcd. C 54.78, H 4.28, N 5.94; found C 54.87, H 4.18, N 5.86. UV/Vis: λ_{max} (MeCN, absorbance) = 365, 272, 230 nm; λ_{max} (solid, reflectance) = 615, 380 nm. IR (KBr): ν = ν_{s+as}(COO[−]) = 1602, 1547, 1376 cm^{−1}, ν(C=N) = 1622 cm^{−1}.

Compound 3: Yield 0.027 g (55%). C₄₄H₄₄CoCu₂N₄O₁₀ (974.86): calcd. C 54.21, H 4.55, N 5.75; found C 54.30, H 4.46, N 5.84. UV/Vis: λ_{max} (MeCN, absorbance) = 365, 271, 230 nm; λ_{max} (solid, reflectance) = 612, 380 nm. IR (KBr): ν = ν_{s+as}(COO[−]) = 1597, 1548, 1379 cm^{−1}, ν(C=N) = 1624 cm^{−1}.

Physical Measurements: Elemental analyses (C, H and N) were performed with a Perkin–Elmer 2400 series II CHN analyzer. IR spectra in KBr pellets (4000–500 cm^{−1}) were recorded with a Perkin–Elmer RXI FTIR spectrophotometer. All solutions were prepared in spectroscopic grade solvents. Electronic spectra were recorded in acetonitrile (800–200 nm) in a 1 cm optical glass cuvette as well as in the solid state (800–300 nm) with a Hitachi U-3501 spectrophotometer, using the appropriate setup. The variable-temperature magnetic susceptibility data of crystalline samples of **1–3** were collected with a Quantum Design superconducting quantum interference device (SQUID) magnetometer at the Serveis Científicotècnics of the Universitat de Barcelona. Pascal’s constants were used to estimate diamagnetic corrections to the molar paramagnetic susceptibility, and a correction was applied for the sample holder.

Crystallographic Data Collection and Refinement: Suitable single crystals of each of the three complexes were mounted with a Bruker-AXS SMART APEX II diffractometer equipped with a graphite monochromator and Mo-K_α (λ = 0.71073 Å) radiation. The crystals were positioned 60 mm from the CCD. 360 frames were measured with a counting time of 10 s. The structures were solved by using the Patterson method with SHELXS 97. Subsequent difference Fourier synthesis and least-square refinement revealed the positions of the remaining non-hydrogen atoms, which were refined with independent anisotropic displacement parameters. However, for complex **1**, the disordered oxygen atom O(100) and O(200) was refined isotropically. Hydrogen atoms were placed in idealized positions and their displacement parameters were fixed to be 1.2 times larger than those of the attached non-hydrogen atom. Successful convergence was indicated by a maximum shift/error of 0.001 for the last cycle of the least-square refinement. The non-ideal data obtained for complex **3** are due to the intrinsic nature of the crystal. Absorption corrections were carried out with the SADABS program.^[36] All calculations were carried out with SHELXS 97,^[37] SHELXL 97,^[38] PLATON 99,^[39] ORTEP-32,^[40] and WinGX system ver-1.64.^[41] Data collection and structure-refinement parameters and crystallographic data for the three complexes are given in Table 3.

CCDC-1052921 (for **1**), -1052922 (for **2**), and -1052923 (for **3**) contain the supplementary crystallographic data for this paper. These data can

Table 3. Parameters for data collection and structure refinement for complexes **1–3**.

	1	2	3
Formula	C ₅₀ H ₄₄ N ₄ O ₁₃ Cu ₂ Co	C ₄₃ H ₄₀ N ₄ O ₉ Cu ₂ Co	C ₄₄ H ₄₄ N ₄ O ₁₀ Cu ₂ Co
Formula weight	1094.92	942.82	974.86
Space group	orthorhombic	monoclinic	monoclinic
Crystal system	<i>Pna</i> 2 ₁	<i>P</i> 2 ₁ / <i>n</i>	<i>P</i> 2 ₁ / <i>c</i>
<i>a</i> [Å]	17.542(2)	10.387(5)	9.360(5)
<i>b</i> [Å]	10.803(1)	18.200(5)	20.213(5)
<i>c</i> [Å]	26.281(3)	21.465(5)	11.452(5)
β [°]	90.0	96.833(5)	113.741(5)
<i>V</i> [Å ³]	4980(1)	4029(2)	1983(1)
<i>Z</i>	4	4	2
<i>D</i> _{calc} [g cm ^{−3}]	1.458	1.554	1.632
μ [mm ^{−1}]	1.243	1.515	1.544
<i>F</i> (000)	2236	1932	1002
<i>R</i> _{int}	0.0610	0.0933	0.0397
θ range [°]	1.0–25.1	1.5–25.1	2.0–24.8
Total reflections	33157	52647	8830
Unique reflections	8756	7172	3264
Data with <i>I</i> > 2σ(<i>I</i>)	6610	5105	2384
<i>R</i> ₁ on <i>I</i> > 2σ(<i>I</i>)	0.0517	0.0807	0.0439
<i>wR</i> ₂ [<i>I</i> > 2σ(<i>I</i>)]	0.1354	0.2081	0.1089
GOF on <i>F</i> ²	1.045	1.148	1.068
Temperature [K]	293	293	293

be obtained free of charge from The Cambridge Crystallographic Data Centre via www.ccdc.cam.ac.uk/data_request/cif.

Supporting Information (see footnote on the first page of this article): Electronic absorption and reflectance spectra of the complexes and the plot of χ_M vs. T and $-J$ vs. Cu–O–Co angles of complexes 1–3.

Acknowledgments

The authors thank the Department of Science and Technology (DST), New Delhi for financial support (grant number SR/S1/IC/0034/2012) as well as for the DST-FIST-funded single-crystal X-ray diffractometer facility at the department of chemistry, University of Calcutta. S. G. is thankful to the University Grants Commission (UGC), New Delhi for a Senior Research Fellowship. P. G. acknowledges the ICREA (Institució Catalana de Recerca i Estudis Avançats) and the Ministerio de Economía y Competitividad (MINECO) of Spain (project numbers CTQ2011-27929-C02-01 and CTQ2012-32247, grants to P. G. and G. A., respectively). G. A. thanks the Generalitat de Catalunya for the prize ICREA Academia 2008 and 2013, for excellence in research and the European Research Council (ERC) for a starting grant (258060 FuncMolQIP).

- [1] a) P. T. Corbett, J. Leclaire, L. Vial, K. R. West, J.-L. Wietor, J. K. M. Sanders, S. Otto, *Chem. Rev.* **2006**, *106*, 3652–3711; b) S. Mann, *Nature* **1993**, *365*, 499–505; c) J.-M. Lehn, *Angew. Chem. Int. Ed.* **2013**, *52*, 2836–2850.
- [2] a) X. Q. Lewell, D. B. Judd, S. P. Watson, M. M. Hann, *J. Chem. Inf. Comput. Sci.* **1998**, *38*, 511–522; b) F. Guiller, D. Orain, M. Bradley, *Chem. Rev.* **2000**, *100*, 2091–2158; c) D. A. Tomalia, *Aldrichim. Acta* **2004**, *37*, 39–57; d) Y.-B. Zhang, H.-L. Zhou, R.-B. Lin, C. Zhang, J.-B. Lin, J.-P. Zhang, X.-M. Chen, *Nat. Commun.* **2012**, *3*, 642; e) R. Robson, *J. Chem. Soc., Dalton Trans.* **2000**, 3735–3744.
- [3] a) G. Férey, *Chem. Soc. Rev.* **2008**, *37*, 191–214; b) C. S. Mahon, D. A. Fulton, *Nat. Chem.* **2014**, *6*, 665–672.
- [4] a) O. M. Yaghi, M. O’Keeffe, N. W. Ockwig, H. K. Chae, M. Eddaoudi, J. Kim, *Nature* **2003**, *423*, 705–714; b) O. K. Farha, A. Ö. Yazaydin, I. Eryazici, C. D. Malliakas, B. G. Hauser, M. G. Kanatzidis, S. T. Nguyen, R. Q. Snurr, J. T. Hupp, *Nat. Chem.* **2010**, *2*, 944–948; c) G. R. Whittell, M. D. Hager, U. S. Schubert, I. Mannes, *Nat. Mater.* **2011**, *10*, 176–188.
- [5] a) Y. E. Alexeev, B. I. Kharisov, T. C. Hernández García, A. D. Garnovskii, *Coord. Chem. Rev.* **2010**, *254*, 794–831; b) M. Andruh, *Chem. Commun.* **2011**, *47*, 3025–3042.
- [6] a) S. R. Batten, K. S. Murray, *Coord. Chem. Rev.* **2003**, *246*, 103–130; b) R. Chakrabarty, P. S. Mukherjee, P. J. Stang, *Chem. Rev.* **2011**, *111*, 6810–6918.
- [7] a) Y.-Z. Zheng, Z. Zheng, X.-M. Chen, *Coord. Chem. Rev.* **2014**, *258*–259, 1–15; b) G. B. Deacon, E. E. Delbridge, C. M. Forsyth, B. W. Skelton, A. H. White, *J. Chem. Soc., Dalton Trans.* **2000**, 745–751; c) P. Pachfule, Y. Chen, S. C. Sahoo, J. Jiang, R. Banerjee, *Chem. Mater.* **2011**, *23*, 2908–2916; d) Y.-Q. Sun, Y.-Y. Xu, D.-Z. Gao, G.-Y. Zhang, Y.-X. Liu, J. Wang, D.-Z. Liao, *Dalton Trans.* **2012**, *41*, 5704–5714.
- [8] a) M. Du, X.-J. Jiang, X.-J. Zhao, *Inorg. Chem.* **2007**, *46*, 3984–3995; b) F.-P. Huang, J.-L. Tian, W. Gu, X. Liu, S.-P. Yan, D.-Z. Liao, P. Cheng, *Cryst. Growth Des.* **2010**, *10*, 1145–1154; c) T. Liu, S. Wang, J. Lu, J. Dou, M. Niu, D. Lia, J. Bai, *CrystEngComm* **2013**, *15*, 5476–5489; d) B. Hu, Y.-G. Wang, Y. Dai, Y.-X. Peng, W. Huang, *Polyhedron* **2014**, *83*, 205–211.
- [9] Y. Go, X. Wang, E. V. Anokhina, A. J. Jacobson, *Inorg. Chem.* **2004**, *43*, 5360–5367.
- [10] a) A. V. Pavlishchuk, S. V. Kolotilov, M. Zeller, L. K. Thompson, A. W. Addison, *Inorg. Chem.* **2014**, *53*, 1320–1330; b) A. D. Cutland, J. A. Halfen, J. W. Kampf, V. L. Pecoraro, *J. Am. Chem. Soc.* **2001**, *123*, 6211–6212.
- [11] a) M. Pascu, F. Lloret, N. Avarvari, M. Julve, M. Andruh, *Inorg. Chem.* **2004**, *43*, 5189–5191; b) D. G. Branzee, A. Guerri, O. Fabelo, C. Ruiz-Pérez, L.-M. Chamoreau, C. Sangregorio, A. Caneschi, M. Andruh, *Cryst. Growth Des.* **2008**, *8*, 941–949.
- [12] a) M. Fondo, A. M. García-Deibe, N. Ocampo, J. Sanmartín, M. R. Bermejo, A. L. Llamas-Saiz, *Dalton Trans.* **2006**, 4260–4270; b) M. Fondo, A. M. García-Deibe, N. Ocampo, J. Sanmartín, M. R. Bermejo, E. Oliveira, C. Lodeiro, *New J. Chem.* **2008**, *32*, 247–257; c) M. Fondo, A. M. García-Deibe, N. Ocampo, J. Sanmartín, *Eur. J. Inorg. Chem.* **2010**, 2376–2384.
- [13] a) S. Ghosh, G. Aromí, P. Gamez, A. Ghosh, *Eur. J. Inorg. Chem.* **2014**, 3341–3349; b) P. Seth, A. Figuerola, J. Jover, E. Ruiz, A. Ghosh, *Inorg. Chem.* **2014**, *53*, 9296–9305.
- [14] a) W. L. Leong, J. J. Vittal, *Chem. Rev.* **2011**, *111*, 688–764; b) J. V. Barth, G. Costantini, K. Kern, *Nature* **2005**, *437*, 671–679.
- [15] L. C. Francesconi, D. R. Corbin, A. W. Claus, D. N. Hendrickson, G. D. Stucky, *Inorg. Chem.* **1981**, *20*, 2078–2083.
- [16] P. Seth, S. Ghosh, A. Figuerola, A. Ghosh, *Dalton Trans.* **2014**, *43*, 990–998.
- [17] a) O. Kahn, *Molecular Magnetism*, Wiley-VCH, Weinheim, Germany, **1993**; b) E. Pardo, R. Ruiz-García, F. Lloret, J. Faus, M. Julve, Y. Journaux, F. Delgado, C. Ruiz-Pérez, *Adv. Mater.* **2004**, *16*, 1597–1600; c) G. E. Kostakis, S. P. Perlepes, V. A. Blatov, D. M. Proserpio, A. K. Powell, *Coord. Chem. Rev.* **2012**, *256*, 1246–1278; d) D. S. Nesterov, V. N. Kokozay, J. Jezierska, O. V. Pavlyuk, R. Boča, A. J. L. Pombeiro, *Inorg. Chem.* **2011**, *50*, 4401–4411.
- [18] a) G. A. Timco, T. B. Faust, F. Tuna, R. E. P. Winpenny, *Chem. Soc. Rev.* **2011**, *40*, 3067–3075; b) M. Kurmoo, *Chem. Soc. Rev.* **2009**, *38*, 1353–1379; c) E. Pardo, R. Ruiz-García, J. Cano, X. Ottenwaelder, R. Lescouëzec, Y. Journaux, F. Lloret, M. Julve, *Dalton Trans.* **2008**, 2780–2805.
- [19] a) J.-P. Costes, R. Gheorghe, M. Andruh, S. Shova, J.-M. Clemente Juan, *New J. Chem.* **2006**, *30*, 572–576; b) D. G. Branzee, A. M. Madalan, S. Ciattini, N. Avarvari, A. Caneschi, M. Andruh, *New J. Chem.* **2010**, *34*, 2479–2490; c) S. Biswas, C. J. Gómez-García, J. M. Clemente-Juan, S. Benmansour, A. Ghosh, *Inorg. Chem.* **2014**, *53*, 2441–2449.
- [20] a) D. Visinescu, A. M. Madalan, M. Andruh, C. Duhayon, J.-P. Sutter, L. Ungur, W. Van den Heuvel, L. F. Chibotaru, *Chem. Eur. J.* **2009**, *15*, 11808–11814; b) Q.-B. Bo, Z.-W. Zhang, J.-L. Miao, D.-Q. Wang, G.-X. Sun, *CrystEngComm* **2011**, *13*, 1765–1767; c) L.-F. Ma, M.-L. Han, J.-H. Qin, L.-Y. Wang, M. Du, *Inorg. Chem.* **2012**, *51*, 9431–9442; d) D. Kim, X. Song, J. H. Yoon, M. S. Lah, *Cryst. Growth Des.* **2012**, *12*, 4186–4193.
- [21] a) S. Biswas, S. Naiya, M. G. B. Drew, C. Estarellas, A. Frontera, A. Ghosh, *Inorg. Chim. Acta* **2011**, *366*, 219–226; b) S. Biswas, A. Ghosh, *Indian J. Chem. Sect. A* **2011**, *50*, 1356–1362; c) S. Ghosh, S. Mukherjee, P. Seth, P. S. Mukherjee, A. Ghosh, *Dalton Trans.* **2013**, *42*, 13554–13564; d) S. Ghosh, Y. Ida, T. Ishida, A. Ghosh, *Cryst. Growth Des.* **2014**, *14*, 2588–2598; e) L. K. Das, A. Ghosh, *CrystEngComm* **2013**, *15*, 9444–9456.
- [22] a) K. Nakamoto, *Infrared and Raman Spectra of Inorganic and Coordination Compounds*, Wiley, New York, 4th ed. **1986**; b) P. Mukherjee, M. G. B. Drew, C. J. Gómez-García, A. Ghosh, *Inorg. Chem.* **2009**, *48*, 5848–5860; c) A. Hazari, L. K. Das, A. Bauzá, A. Frontera, A. Ghosh, *Dalton Trans.* **2014**, *43*, 8007–8015.
- [23] A. W. Addison, T. N. Rao, J. Reedijk, J. van Rijn, G. C. Verschoor, *J. Chem. Soc., Dalton Trans.* **1984**, 1349–1356.
- [24] W.-H. Zhang, Y.-L. Song, Z.-H. Wei, L.-L. Li, Y.-J. Huang, Y. Zhang, J.-P. Lang, *Inorg. Chem.* **2008**, *47*, 5332–5346.
- [25] P.-K. Chen, Y.-X. Che, J.-M. Zheng, S. R. Batten, *Chem. Mater.* **2007**, *19*, 2162–2167.
- [26] M. T. Ng, T. C. Deivaraj, J. J. Vittal, *Inorg. Chim. Acta* **2003**, *348*, 173–178.
- [27] a) T. Shimogaki, S. Dei, K. Ohtab, A. Matsumoto, *J. Mater. Chem.* **2011**, *21*, 10730–10737; b) A. Motoshige, Y. Mawatari, Y. Yoshida, R. Motoshige, M. Tabata, *Polym. Chem.* **2014**, *5*, 971–978; c) M. Sereydyuk, A. B. Gaspar, V. Ksenofontov, Y. Galyametdinov, M. Verdaguer, F. Villain, P. Gülich, *Inorg. Chem.* **2008**, *47*, 10232–10245.

- [28] a) A. M. Kirillov, Y. Y. Karabach, M. Haukka, M. F. C. Guedes da Silva, J. Sanchiz, M. N. Kopylovich, A. J. L. Pombeiro, *Inorg. Chem.* **2008**, *47*, 162–175; b) K. R. Gruenwald, A. M. Kirillov, M. Haukka, J. Sanchiz, A. J. L. Pombeiro, *Dalton Trans.* **2009**, 2109–2120; c) P. Seppälä, E. Colacio, A. J. Mota, R. Sillanpää, *Inorg. Chim. Acta* **2010**, *363*, 755–762.
- [29] a) J. Chakraborty, M. Nandi, H. Mayer-Figge, W. S. Sheldrick, L. Sorace, A. Bhaumik, P. Banerjee, *Eur. J. Inorg. Chem.* **2007**, 5033–5044; b) H.-H. Chen, Y.-Y. Liu, *Z. Kristallogr. New Cryst. Struct.* **2010**, *225*, 433–436.
- [30] M. Pascu, M. Andruh, A. Müller, M. Schmidtman, *Polyhedron* **2004**, *23*, 673–678.
- [31] a) X.-P. Yang, R. A. Jones, W.-K. Wong, V. Lynch, M. M. Oye, A. L. Holmes, *Chem. Commun.* **2006**, 1836–1838; b) R. Gheorghe, P. Cucos, M. Andruh, J.-P. Costes, B. Donnadieu, S. Shova, *Chem. Eur. J.* **2006**, *12*, 187–203.
- [32] N. F. Chilton, R. P. Anderson, L. D. Turner, A. Soncini, K. S. Murray, *J. Comput. Chem.* **2013**, *34*, 1164–1175.
- [33] F. Lloret, M. Julve, J. Cano, R. Ruiz-García, E. Pardo, *Inorg. Chim. Acta* **2008**, *361*, 3432–3445.
- [34] Y.-Z. Zhang, A. J. Brown, Y.-S. Meng, H.-L. Sun, S. Gao, *Dalton Trans.* **2015**, *44*, 2865–2870.
- [35] S. Ghosh, S. Biswas, A. Bauzá, M. Barceló-Oliver, A. Frontera, A. Ghosh, *Inorg. Chem.* **2013**, *52*, 7508–7523.
- [36] *SAINT*, v. 6.02 and *SADABS*, v. 2.03, Bruker AXS, Inc., Madison WI, **2002**.
- [37] G. M. Sheldrick, *SHELXS 97, Program for Structure Solution*, University of Göttingen, Germany, **1997**.
- [38] G. M. Sheldrick, *SHELXL 97, Program for Crystal Structure Refinement*, University of Göttingen, Germany, **1997**.
- [39] A. L. Spek, *J. Appl. Crystallogr.* **2003**, *36*, 7–13.
- [40] L. J. Farrugia, *J. Appl. Crystallogr.* **1997**, *30*, 565.
- [41] L. J. Farrugia, *J. Appl. Crystallogr.* **1999**, *32*, 837–838.

Received: March 11, 2015
Published Online: June 2, 2015